

Verification of the interaction between peptide T and CD4 using surface plasmon resonance

Tracie E. Ramsdale^{a,*}, Peter R. Andrews^a, Edouard C. Nice^b

^aCentre for Drug Design and Development, University of Queensland, St. Lucia, 4072, Australia

^bLudwig Institute for Cancer Research, Melbourne Branch, P.O. Royal Melbourne Hospital, Victoria 3050, Australia

Received 28 April 1993; revised version received 13 September 1993

Peptide T is currently in phase II clinical trials for the treatment of AIDS-associated dementia. Its putative mode of action is inhibition of binding of the HIV envelope protein (gp120) to its cellular receptor (CD4), thus preventing viral infectivity and gp120-induced neuronal toxicity. However, a number of reports have appeared in the literature which have failed to observe any inhibitory activity of Peptide T on CD4-gp120 binding, thus casting doubt on this hypothesis. This study uses a novel biosensor technique to demonstrate that Peptide T does bind to CD4 and that this binding can be specifically inhibited by an anti-CD4 monoclonal antibody. A detailed analysis of the kinetics of the interaction is presented.

Peptide T; Surface plasmon resonance; Biosensor; AIDS-associated dementia; Kinetics

1. INTRODUCTION

Peptide T (D-ala¹-STTTNYT amide) is currently in phase II clinical trials for treatment of AIDS-associated neurocognitive impairment [1].

The peptide was originally derived from an octapeptide sequence (ASTTTNYT) of the envelope glycoprotein (gp120) of the ARV2 isolate of HIV and was shown by Pert et al. to be a potent inhibitor of [¹²⁵I]gp120 binding to T4 on rat brain membranes [2]. Furthermore, HIV infection of human T cells was antagonized by low (0.1 nM) concentrations of the peptide [2].

Pert and co-workers also noted a sequence similarity between peptide T and vasoactive intestinal peptide (VIP: residues 7–11), and have shown that both peptides are potent agonists of human monocyte chemotaxis. This interaction is specifically inhibited by anti-CD4 monoclonal antibodies (MAbs) but not other mononuclear cell MAbs, leading Pert to suggest that VIP may be the endogenous neuropeptide for the CD4 receptor [3]. In support of this hypothesis, it was demonstrated that tritiated Peptide T binding to rat brain membranes can be inhibited by both gp120 and VIP [4].

This relationship between Peptide T, VIP, CD4 and gp120 is consistent with the observed therapeutic benefits of Peptide T in the treatment of AIDS-associated dementia, which appears to result less from viral infection than from a direct neurotoxic action of gp120 itself [5]. Thus, Pert et al. have not only demonstrated gp120-

induced neuronal cell death, but have also shown that it can be specifically prevented by anti-CD4 monoclonal antibodies, VIP, Peptide T and related Peptide T structures from various HIV isolates [6,7]. Pert et al. explained the above findings by suggesting that the T4 receptor found in human brain is normally modulated by VIP and that HIV, or more precisely the envelope glycoprotein of HIV, mimics VIP binding via peptide T (4–8), a pentapeptide found in approximately the same region of all sequenced HIV isolates. AIDS-associated dementia then results from the interference of gp120 with normal VIP-ergic neurotrophic effects and effects on cerebral blood flow [8].

Despite this impressive array of evidence, Pert's hypothesis has been under continuous attack since 1987 when a number of investigators reported their inability to demonstrate any anti-HIV effects of Peptide T under various experimental conditions [9,10]. In support of Pert, others claim to have confirmed the original work [11] and a possible explanation has been advanced to account for the contradictory findings [12]. The potent chemotactic activity of peptide T and related analogs in human monocytes has also been confirmed in other laboratories [13,14]. Most damning of all, however, is a recently published paper [15] which asserts categorically that Peptide T does not bind to CD4.

Thus, despite the favorable outlook for Peptide T in AIDS therapy, the controversy over its mode of action remains unresolved.

In this paper we address the following:

1. Reinvestigate the binding of Peptide T to CD4, using the newly developed detection phenomenon of surface plasmon resonance (SPR) [16–18];
2. Demonstrate that Peptide T unquestionably does

*Corresponding author. Fax: (61) (7) 365 1990.

Abbreviations: VIP, vasoactive intestinal peptide; SPR, surface plasmon resonance; BIA, biospecific interaction analysis; RU, response units; sCD4, soluble CD4.

bind to CD4 and that this binding can be specifically inhibited by an anti-CD4 monoclonal antibody;

3. Offer explanations for the failure of other's to confirm Pert's observations, and some guidelines for avoiding similar pitfalls in the future.

2. MATERIALS AND METHODS

2.1. Surface plasmon resonance

The phenomenon of surface plasmon resonance [19] enables monitoring of macromolecular interactions in real time. The biosensor employed in this study (Pharmacia BIAcore) uses a sensor chip comprising a glass slide coated with a thin film of gold. Light is focussed on the gold surface of the sensor chip in a wedge shaped beam giving a fixed range of incident angles. Above a certain critical angle of incidence, total internal reflection is observed. Under these conditions, an electromagnetic field component termed the evanescent wave penetrates a short distance into the medium of lower refractive index. This wave is amplified by resonant oscillation of delocalized electrons (or plasmons) in the metal film. This phenomenon is termed surface plasmon resonance. At a specific incident angle, which is dependent on the refractive indices of the media, a sharp dip in the intensity of reflected light appears. The angle at which this occurs is known as the SPR angle.

In BIAcore, the sensor chip forms one wall of a thin layer flow cell. As the refractive index of the solution in contact with the surface changes, the displacement of the SPR angle is recorded in real time as a sensorgram, and is quantified as response units, RU. The gold film on the sensor chip surface in contact with the flow path is covered with a carboxymethylated dextran hydrogel, to which biomolecules can be coupled using standard coupling chemistry. Thus one component (ligand) of the interaction is immobilised on the surface. The other component (analyte) is allowed to flow over the sensor surface in solution. The change in SPR angle is directly related to the change in surface concentration of analyte. A response of 1000 RU corresponds to a shift of 0.1° in the resonance angle, which in turn represents a change in surface protein concentration of about 1 ng/mm^2 or in bulk refractive index of about 10^{-3} [20].

2.2. Instrumentation and reagents

The BIAcore system and reagents including sensor chips CM5, surfactant P20 and the amine coupling kit containing *N*-hydroxysuccinimide (NHS), *N*-ethyl-*N'*-(3-diethylaminopropyl) carbodiimide (EDC) and ethanolamine hydrochloride were obtained from Pharmacia Biosensor AB, Uppsala, Sweden. Human sCD4 was obtained from Du Pont, E.I. DuPont de Nemours, Medical Products Dept, Boston, USA. T4 monoclonal antibody (SFC112T4D11) was obtained from Coulter Immunology, Hialeah, FL, USA. Peptide T and VIP (residues 5–12) were gifts from Auspep Pty. Ltd., West Melbourne, Australia (homogeneity was verified by HPLC and mass spectrometry). The buffer used for all experiments was HBS (10 mM HEPES, 3.4 mM EDTA, 150 mM NaCl, 0.05% surfactant P20, pH 7.4).

2.3. Immobilisation of ligands onto sensor surfaces

Immobilisation of ligands (sCD4 or Peptide T) was performed as follows. After equilibration with HBS, the automatic robotics injection unit incorporated into the BIAcore instrument was programmed to perform the following injections.

- (i) Equal volumes of NHS (70 μl , 0.1 M in water) and EDC (70 μl , 0.1 M in water) were first mixed by the robot after which 35 μl was injected across the surface to activate the carboxymethylated dextran surface.
- (ii) Ligand (50 μl , 100 $\mu\text{g/ml}$ Peptide T in 10 mM sodium acetate, pH 4.5, or 50 μl , 30 $\mu\text{g/ml}$ sCD4 in 10 mM sodium acetate, pH 4.5) was then injected across the activated surface.
- (iii) Residual NHS esters were inactivated with ethanolamine (35 μl , 1 M in water, pH 8.5).

- (iv) Noncovalently bound ligand was then washed from the surface by injecting hydrochloric acid (10 μl , 0.1 M).

The immobilisation protocol was performed with a continuous flow of HBS of 4 $\mu\text{l/min}$. A representative sensorgram obtained during the immobilisation of peptide T is shown in Fig. 1.

2.4. Binding assays and data analysis

Each binding cycle was performed with a constant flow of HBS of 2 $\mu\text{l/min}$. Samples of analyte, prepared in HBS, were injected across the surface via a sample loop contained within the fluidics cartridge of the system. Once the sample injection was complete, the surface was regenerated by injection of 10 mM HCl. Analyte binding was measured as the increase in the SPR signal of the immobilised ligand layer with HBS flow before and after injection of analyte. Inhibition studies were carried out by co-incubating the inhibitor with analyte for 30 min at room temperature prior to injection.

2.5. Theory of kinetic measurements

To apply the general rate equation [21,22] to the formation of AB complexes, the progress of the reaction must be monitored. This is usually achieved by determination of the concentration of the complex or either of the reactants at known times. For example, the concentration of reactant B is given by:

$$[B]_t = [B]_0 - [AB]_t$$

where $[B]_0$ is the initial concentration of reactant B at time 0.

Substitution in to the general rate equation for the formation of complex AB yields:

$$\frac{d[AB]}{dt} = k_{\text{ass}} [A]_t ([B]_0 - [AB]_t) - k_{\text{diss}} [AB]_t$$

In real-time biospecific interaction analysis (BIA), complex formation is monitored directly as the change in response (R) with time. The concentration of free analyte is kept constant through a continuous flow of fresh analyte solution past the sensor surface. Denoting the analyte as A (concentration C) and the ligand as B gives

$$\frac{dR}{dt} = k_{\text{ass}} C (R_{\text{max}} - R_t) - k_{\text{diss}} R_t \quad (\text{Eqn. 1})$$

where C is the concentration of free analyte in solution; R_{max} is the total amount of binding sites of the immobilised ligand B expressed as SPR response in RU; $R_{\text{max}} - R_t$ is the amount of remaining free binding sites at time t expressed as SPR response in RU; dR/dt is the rate of formation of surface complexes expressed as SPR response in $\text{RU} \cdot \text{s}^{-1}$, i.e. the derivative of the response curve.

2.5.1. Association

Rearrangement of the above equation clearly shows that the derivative of the binding curve is linearly related to the response. Thus rate constants can be derived from a plot of dR/dt versus R :

$$\frac{dR}{dt} = k_{\text{ass}} C R_{\text{max}} - (k_{\text{ass}} C + k_{\text{diss}}) R_t \quad (\text{Eqn. 2})$$

The problem with this approach is that one needs to know R_{max} , the response obtained for saturation of the immobilised ligand. This can, in principle, be determined by injecting a saturating concentration of analyte. However, this requires very high analyte concentrations and is thus unrealistic if precious samples are involved.

Examination of Eqn. 2 reveals that the slope ($k_{\text{ass}} C + k_{\text{diss}}$) of the line obtained by plotting dR/dt against R is itself linearly related to the concentration of free analyte C . Hence a plot of the slopes of the dR/dt vs. R lines as a function of analyte concentration C , yields a new line with slope k_{ass} and intercept on the abscissa k_{diss} .

2.5.2. Dissociation

After the sample pulse is complete, the concentration of free analyte suddenly drops to zero. The derivative of the response curve then

reflects the dissociation rate, assuming that re-association of released analyte is negligible:

$$\frac{dR}{dt} = -k_{\text{diss}} R_t \quad (\text{Eqn. 3})$$

Integrating with respect to times gives:

$$\ln \frac{R_{t_1}}{R_{t_n}} = k_{\text{diss}} (t_n - t_1) \quad (\text{Eqn. 4})$$

where R_{t_n} is the response at time n and R_{t_1} is the response at an arbitrary starting time t_1 . The dissociation rate constant k_{diss} can thus be obtained by plotting the log of drop in response against time interval.

2.6. Kinetics runs

sCD4 at concentrations ranging from 10 $\mu\text{g/ml}$ to 60 $\mu\text{g/ml}$ in HBS was allowed to interact with Peptide T immobilised on the sensor surface. The runs were performed at 25°C, at a flow rate of 2 $\mu\text{l/min}$ during 25 min (50 μl injection), taking report points every 20 s. The complex was then allowed to dissociate for 1200 s using a continuous flow of buffer at a rate of 2 $\mu\text{l/min}$. Report points were taken every 50 s. The surface was regenerated with 10 mM HCl over 2.5 min (flow rate 50 $\mu\text{l/min}$). The BIAcore software produces a report point table which can be analysed directly in Microsoft Excel.

3. RESULTS AND DISCUSSION

3.1. Ligand immobilisation

Fig. 1 illustrates the immobilisation of Peptide T onto the sensor surface. The 639 RU difference between report points 1 and 2 corresponds to immobilised peptide, and is equivalent to a surface concentration of approximately 0.6 ng/mm^2 [23]. A similar sensorgram was obtained for the immobilisation of sCD4 (50 μl , 35 $\mu\text{g/ml}$, other conditions as stated for peptide T immobilisation) with 6973 RU of ligand being immobilised. The greater response is due, in part, to the larger molecular weight of sCD4 (apparent molecular weight 45,000 Da) as compared with Peptide T (858 Da).

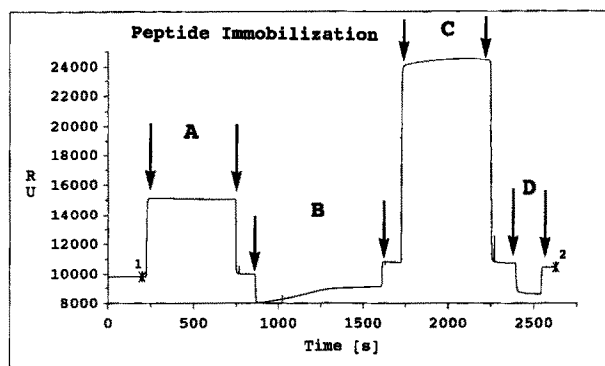


Fig. 1. Sensorgram obtained for the immobilisation of Peptide T. The flow rate is 4 $\mu\text{l/min}$. The beginning and end of injections are indicated by arrows. The large differences in RU at the beginning and end of injections are due to differences in the refractive indices of the injected material and the buffer. The injections performed are (A) activation of the carboxylated dextran matrix by injection of 35 μl of EDC/NHS mixture, (b) injection of 50 μl of 100 $\mu\text{g/ml}$ of Peptide T in sodium acetate, pH 4.5, (C) inactivation of unreacted esters by ethanolamine, (D) washing off noncovalently bound peptide with 50 μl of 10 mM HCl.

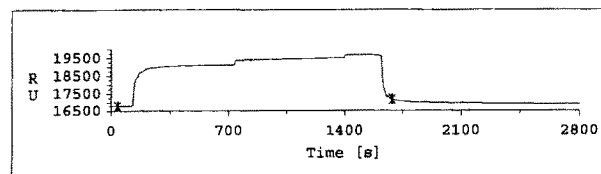


Fig. 2. Sensorgram illustrating binding of Peptide T (50 μl , 10 $\mu\text{g/ml}$) to immobilised sCD4, at a flow rate of 2 $\mu\text{l/min}$. Amount of analyte bound is determined by the difference in response before and after the injection, i.e. 382 RU.

3.2. Peptide and monoclonal antibody binding to immobilised sCD4

Fig. 2 shows a representative sensorgram obtained upon injection of Peptide T (50 μl , 10 mg/ml) across the immobilised sCD4 surface. The amount of analyte bound is measured as the difference between response before and after the injection, i.e. between report points 1 and 2. In this case, a total of 382 RU was obtained. A similar response was observed for the VIP fragment (residues 5–12, 50 μl , 10 mg/ml), with a total increase of 372 RU. This indicates that both Peptide T and the VIP fragment bind to CD4.

The specificity of this interaction was demonstrated by inhibition of the binding of the anti-CD4 monoclonal antibody, T4 (50 μl , 0.125 $\mu\text{g/ml}$), to immobilised sCD4 (Fig. 3a). This was completely inhibited by pre-incubation with Peptide T (1 mg/ml) (Fig. 3b), suggesting that Peptide T binds to sCD4 at the same site as the monoclonal antibody T4.

3.3. sCD4 binding to immobilised peptide T

Fig. 4 shows representative sensorgrams of the binding of sCD4 (10, 21, 35, 60 $\mu\text{g/ml}$) to immobilised Peptide T. The amount of analyte bound to the surface was 100, 152, 207, 247 RU for 10, 21, 35 and 60 $\mu\text{g/ml}$ concentrations of sCD4, respectively.

Fig. 5 shows the corresponding sensorgram of the binding of sCD4 (10 $\mu\text{g/ml}$) after incubation with T4 monoclonal antibody (0.125 $\mu\text{g/ml}$). The response is

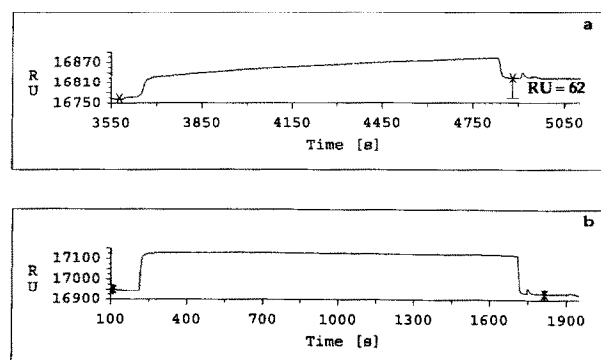


Fig. 3. (a) Sensorgram obtained for binding of T4 MAb (50 μl , 0.125 $\mu\text{g/ml}$) to immobilised sCD4. Flow rate = 2 $\mu\text{l/min}$. (b) Sensorgram obtained for binding of T4 MAb (50 μl , 0.125 $\mu\text{g/ml}$) to immobilised sCD4, after co-incubation with Peptide T (1 mg/ml) for 30 min at room temperature. Flow rate = 2 $\mu\text{l/min}$.

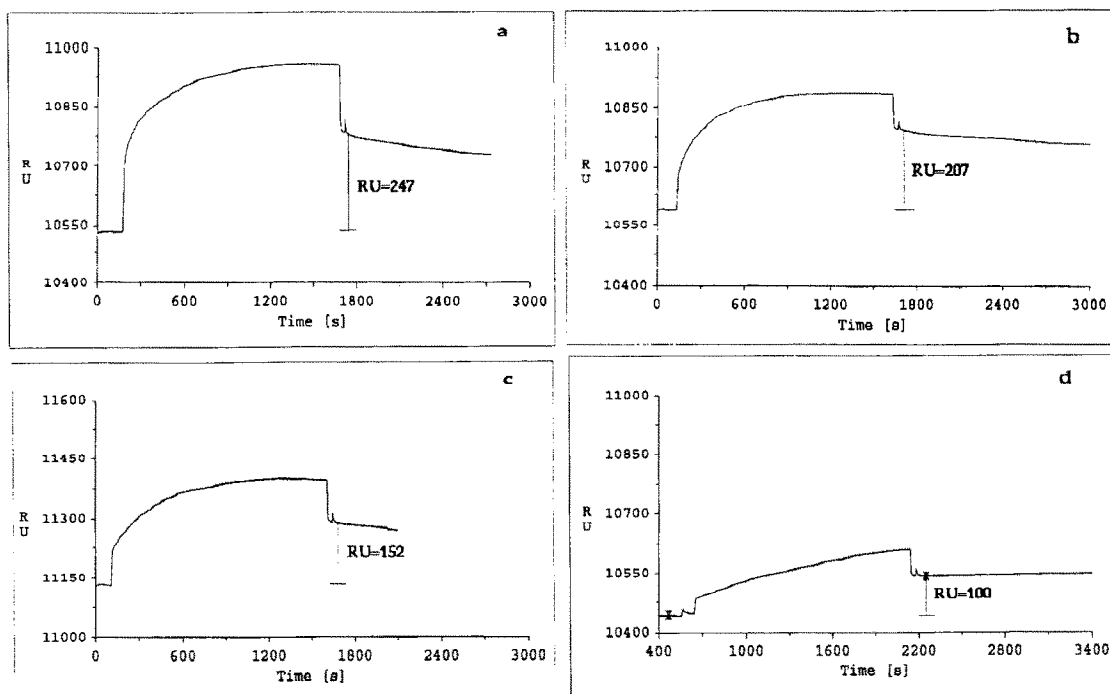


Fig. 4. Sensorgrams obtained for binding of soluble sCD4 to immobilised Peptide T. Flow rate = 2 $\mu\text{l}/\text{min}$. 50 μl injections of the following concentrations were made. Sensorgrams are illustrated in the corresponding panels: (a) 60 $\mu\text{g}/\text{ml}$; (b) 35 $\mu\text{g}/\text{ml}$; (c) 21 $\mu\text{g}/\text{ml}$; (d) 10 $\mu\text{g}/\text{ml}$.

now greatly reduced, i.e. only 26 RU of analyte bound as compared with 100 RU in the absence of T4. This indicates that T4 monoclonal antibody inhibits the

binding of sCD4 to peptide T. As shown earlier (Fig. 3), Peptide T was also able to inhibit the binding of this MAb to sCD4. Since the T4 monoclonal is known to be specific for the gp120 binding site of sCD4, this indicates that peptide T also binds to CD4 in this region.

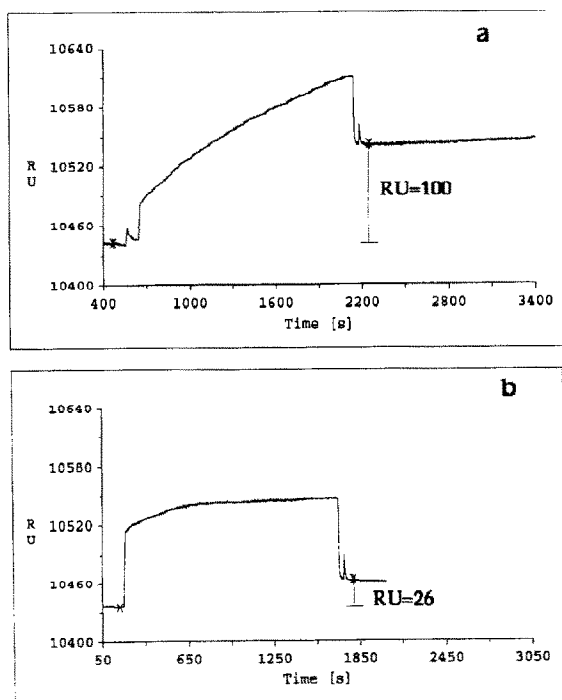


Fig. 5. (a) Sensorgram obtained upon binding of sCD4 (50 μl , 10 $\mu\text{g}/\text{ml}$) to immobilised Peptide T. Flow rate = 2 $\mu\text{l}/\text{min}$. (b) Sensorgram obtained upon binding of sCD4 (50 μl , 10 $\mu\text{g}/\text{ml}$) to immobilised Peptide T, after co-incubation with T4 MAb for 30 min at room temperature. Flow rate = 2 $\mu\text{l}/\text{min}$.

3.4. Kinetics analysis of sCD4-peptide T interaction

Plots of dR/dt vs. R for the four different concentrations (10, 21, 35 and 60 $\mu\text{g}/\text{ml}$) of sCD4 binding to immobilised peptide T (illustrated in Fig. 4) yielded slopes of 0.002224 ($r = 0.992$), 0.003029 ($r = 0.969$), 0.004628 ($r = 0.986$) and 0.007473 ($r = 0.979$), respectively (Fig. 6a). Fig. 6b shows a plot of these derived slopes versus analyte concentration. The slope of this plot yields an apparent association rate constant of 4820 $\text{M}^{-1} \cdot \text{s}^{-1}$ ($r = 0.997$).

Dissociation constants were calculated according to Eqn. 4. A representative plot for the dissociation of sCD4 (35 $\mu\text{g}/\text{ml}$) from immobilised Peptide T is shown in Fig. 7. The dissociation plot is not linear, but appears to comprise an initial rapid dissociation ($k_{\text{diss}} = 2.3 \times 10^{-4} \text{ s}^{-1}$), followed by a slower dissociation phase ($k_{\text{diss}} = 9.5 \times 10^{-5} \text{ s}^{-1}$). Such phenomena have been noted previously and could be expected if the binding is multivalent, if the ligand is heterogeneous or if the immobilisation has caused the ligand to appear heterogeneous [24]. Also rebinding of newly dissociated analyte is possible, especially if the number of available binding sites is high [25]. The initial dissociation rates obtained with the 21 $\mu\text{g}/\text{ml}$ and 60 $\mu\text{g}/\text{ml}$ injections (Fig. 4b and d) of sCD4 were comparable, yielding apparent

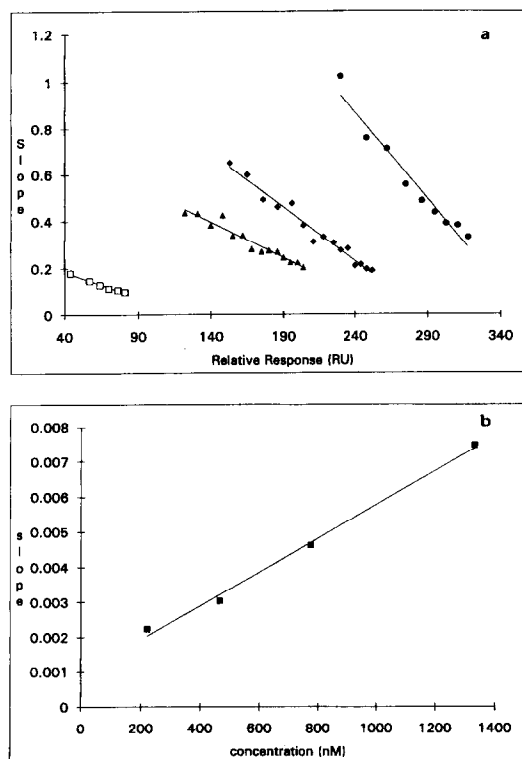


Fig. 6. (a) Slope vs. response for the association phase of sCD4 binding to Peptide T, obtained from sensorgrams shown in Fig. 4. Report points were taken every 20 s, \square , 10 $\mu\text{g/ml}$; \blacktriangle , 21 $\mu\text{g/ml}$; \blacklozenge , 35 $\mu\text{g/ml}$; \bullet , 60 $\mu\text{g/ml}$. (b) Plot of slopes derived from Fig. 6a vs. sCD4 concentration.

dissociation constants of $2.6 \times 10^{-4} \text{ s}^{-1}$ and $3.3 \times 10^{-4} \text{ s}^{-1}$, respectively. Analysis of the dissociation plot shown in Fig. 7 revealed that approximately 8% of the ligand dissociates at the faster rate, with a further 24% dissociating at the slower rate over the remaining time period measured. However, it should be noted that the lowest concentration of sCD4 (10 $\mu\text{g/ml}$, Fig. 4a) failed to show any observable dissociation even after 3000 s. This is indicative of a dissociation rate of 10^{-6} s^{-1} or greater [26].

Using the ratio of the apparent association rate, $4820 \text{ M}^{-1} \cdot \text{s}^{-1}$ and the measurable dissociation rates, 2.7×10^{-4} (average value) and $9.5 \times 10^{-5} \text{ s}^{-1}$, K_d 's of 20 and 56 nM were obtained.

4. CONCLUSION

Using novel biosensor technology, we have demonstrated that

- (i) Peptide T does indeed bind to CD4, with an apparent association rate of $4820 \text{ M}^{-1} \cdot \text{s}^{-1}$ and two apparent dissociation rates of $9.5 \times 10^{-5} \text{ s}^{-1}$ and $2.7 \times 10^{-4} \text{ s}^{-1}$, giving K_d 's of 20 nM and 56 nM, respectively.
- (ii) the binding of peptide T to CD4 can be inhibited

by the monoclonal antibody T4. This antibody is directed to the gp120 binding site of CD4 and is known to inhibit the binding of gp120 to CD4. Inhibition of peptide T binding by MAb T4 thus suggests that peptide T may bind at the same site as gp120.

- (iii) VIP (residues 5–12) also binds to CD4, apparently at the same site. This is of importance as it provides a possible mechanism of action for the observed neurological benefits of peptide T that have been observed in AIDS patients. The data presented here suggest that peptide T and VIP (residues 5–12) bind to CD4 thus supporting the hypothesis of Brenneman et al. that peptide T prevents neuronal cell death by inhibiting the binding of neurotoxic gp120.

In summary, our findings support the original hypotheses of Pert and co-workers that Peptide T and the VIP fragment (residues 5–12) bind to CD4 with high affinity and that this binding can be inhibited by a monoclonal antibody known to prevent gp120 binding. The contradictory reports in the literature may be due, at least in part, to labelling of ligands which interfere with the interaction under investigation. In particular, the most recently published paper refuting the interaction of Peptide T and CD4 [15] uses iodinated Peptide T. Pert et al. had previously shown that tyrosine-7 of Peptide T is crucial for activity and that iodination of this residue abolished activity [27]. It is interesting to note that the only other non-conflicting studies in the literature are those involving chemotaxis assays, which do not require the use of labelled ligands. However, such assays do not allow the detailed analysis of interaction kinetics presented here. It is hoped that this study will

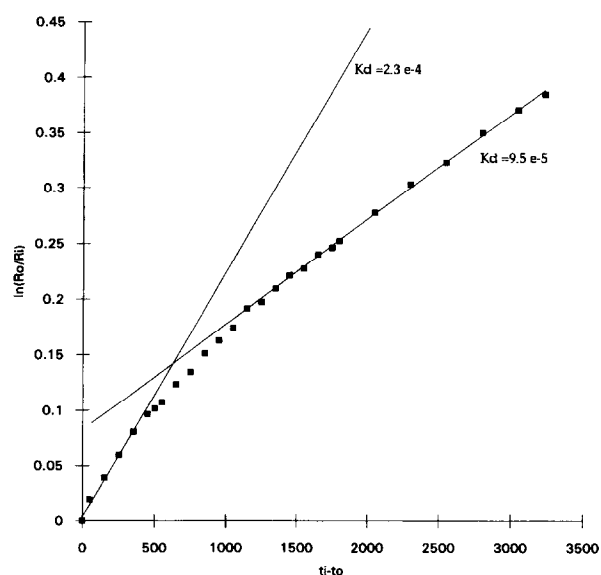


Fig. 7. Dissociation phase plot illustrating the kinetics of dissociation for sCD4 (35 $\mu\text{g/ml}$) from immobilised Peptide T. Apparent dissociation constants, K_d 's were calculated from the slopes of the two lines, as indicated.

assist to dispel the controversy that has arisen surrounding Peptide T and its mode of action.

REFERENCES

- [1] AIDS Medicines in Development: Drugs and Vaccines. Pharmaceutical Manufacturer's Association (1991).
- [2] Pert, C.B., Hill, J.M., Ruff, M.R., Berman, R.M., Robey, W.G., Arthur, L.O., Ruscetti, F.W. and Farrar, W.L. (1986) *Proc. Natl. Acad. Sci. USA* 83, 9254-9258.
- [3] Ruff, M.R., Martin, B.M., Ginns, E.I., Farrar, W.L. and Pert, C.B. (1987) *FEBS Lett.* 211, 17-22.
- [4] Smith, C.C., Hallberg, P.L., Sacerdote, P., Williams, P., Sternberg, E.M., Martin, B.M., Pert, C.B. and Ruff, M.R. (1988) *Drug Dev. Res.* 15, 371-379.
- [5] Glowa, J.R., Panlilio, L.V., Brenneman, D.E., Gozes, I., Fridkin, M. and Hill, J.M. (1992) *Brain Res.* 570, 49-53.
- [6] Brenneman, D.E., Westbrook, G., Fitzgerald, S.P., Ennist, D.L., Elkins, K.L., Ruff, M. and Pert, C.B. (1988) *Nature* 335, 639-642.
- [7] Brenneman, D.E., Buzy, J.M., Ruff, M.R. and Pert, C.B. (1988) *Drug Dev. Res.* 15, 361-369.
- [8] Pert, C.B., Smith, C.C., Ruff, M.R. and Hill, J.M. (1988) *Ann. Neurol.*, Supplement to Volume 23, S71-S73.
- [9] Haseltine, W., Sodroski, J., Kowalski, M., Dorfman, T., Basiripour, L. and Rosen, C. (1987) *The Lancet*, June 20, 1428-1429.
- [10] Clumeck, N. and Hermans, P. (1988) *Am. J. Med.* 85, 165-172.
- [11] Newmark, P. (1987) *Nature*, 327, 449.
- [12] Ruff, M.R., Hallberg, P.L., Hill, J.M. and Pert, C.B. (1987) *The Lancet*, September 26, 751.
- [13] Marastoni, M., Salvadori, S., Balboni, G., Spisani, S., Gavioli, R., Traniello, S. and Tomatis, R. (1990) *Int. J. Peptide Protein Res.* 35, 81-88.
- [14] Marastoni, M., Salvadori, S., Balboni, G., Scaranari, V., Spisani, S., Reali, E., Giuliani, A.L. and Tomatis, R. (1992) *Eur. J. Med. Chem.* 27, 383-393.
- [15] Van den Heever, L.H., Jordaan, J.H. and Dubery, I.A. (1992) *Int. J. Biochem.* 24, 337-339.
- [16] Malmqvist, M. (1993) *Nature* 361, 186-187.
- [17] Fägerstam, L. (1991) in: *Techniques in Protein Chemistry II*, pp. 65-71, Academic Press, New York.
- [18] Jönsson, U. and Malmqvist, M. (1992) in: *Advances in Biosensors* (Turner, A.P.F., Ed.) Vol. 2, pp. 291-336, JAI Press, London.
- [19] Liedberg, B., Nylander, C. and Lundström, I. (1983) *Sensors Actuators* 4, 299-304.
- [20] Löfas, S. and Johnsson, B. (1990) *J. Chem. Soc., Chem. Commun.* 21, 1526-1528.
- [21] Azimzede, A. and Van Regenmortel, M.H.V. (1990) *J. Mol. Recog.* 3, 108-116.
- [22] Altschuh, D., Dubs, M.-C., Weiss, E., Zeder-Lutz, G. and Van Regenmortel, M.H.V. (1992) *Biochemistry* 31, 6298-6304.
- [23] Sterberg, E., Persson, B., Roos, H. and Urbaniczky, C. (1991) *J. Colloid Interface Sci.* 143, 513-526.
- [24] Fagerstam et al. (1992) *J. Chromatogr.* 597, 397-410.
- [25] Felder, S., Zhou, M., Hu, P., Urena, J., Ullrich, A., Chaudhuri, M., White, M., Shoelson, S.E. and Schlessinger, J. (1993) *Mol. Cell Biol.* 13, 1449-1455.
- [26] Borrebaeck, C.A.K., Malmberg, A.-C., Furebring, C., Michaëlson, A., Ward, S. and Ohlin, M. (1992) *Biotechnology* 10, 697-698.
- [27] Sacerdote, P., Ruff, M.R. and Pert, C.B. (1987) *J. Neurosci. Res.* 18, 102-107.